



Published in final edited form as:

Biochem Biophys Res Commun. 2010 September 3; 399(4): 537–541. doi:10.1016/j.bbrc.2010.07.105.

Variable Loss of Kir4.1 channel Function In SeSAME Syndrome Mutations

Xiaofang Tang, Darwin Hang, Andrea Sand, and Paulo Kofuji

Department of Neuroscience, University of Minnesota, Minneapolis, Minnesota

Abstract

SeSAME syndrome is a complex disease characterized by seizures, sensorineural deafness, ataxia, mental retardation, and electrolyte imbalance. Mutations in the inwardly rectifying potassium channel Kir4.1 (*KCNJ10* gene) have been linked to this condition. Kir4.1 channels are weakly rectifying channels expressed in glia, kidney, cochlea and possibly other tissues. We determined the electrophysiological properties of SeSAME mutant channels after expression in transfected mammalian cells. We found that a majority of mutations (R297C, C140R, R199X, T164I) resulted in complete loss of Kir4.1 channel function while two mutations (R65P and A167V) produced partial loss of function. All mutant channels were rescued upon co-transfection of wild-type Kir4.1 but not Kir5.1 channels. Cell surface biotinylation assays indicate significant plasma membrane expression of all mutant channels with exception of the non-sense mutant R199X. These results indicate the differential loss of Kir channel function among SeSAME syndrome mutations.

Keywords

KCNJ10; Glia; Kir4.1; SeSAME Syndrome; EAST syndrome

INTRODUCTION

The biophysical fingerprint of Kir channels is inward rectification in the current-voltage relationship, which limits K⁺ efflux at depolarizing membrane potentials [1;2;3]. By virtue of their functional properties, Kir channels are essential in control of resting membrane potential, coupling of the metabolic cellular state with membrane excitability, and maintenance of K⁺ homeostasis in diverse cell types. Kir4.1 channels encoded by the *KCNJ10* gene are moderately rectifying K⁺ channels with expression in the nervous system, inner ear, and in the kidney [4;5;6;7;8;9]. Previous work has shown that Kir4.1 channel is the principal K⁺ channel expressed in glial cells such as retinal Müller cells, brain astrocytes and satellite glial cells [10;11;12;13;14;15]. Moreover, we and others have found that loss of Kir4.1 channel expression in mice leads to profound glial cell membrane depolarization, impaired extracellular K⁺ buffering, and abnormal neuronal activity in the retina and brainstem [15;16]. The SeSAME (or EAST) syndrome is characterized by seizures, sensorineural deafness, ataxia, mental retardation, and electrolyte imbalances and has been mapped to missense or nonsense mutations in the *KCNJ10* gene [17;18]. Functional consequences of SeSAME mutations likely involve the partial or total loss of Kir4.1 channel

Address for correspondence: Paulo Kofuji, Department of Neuroscience, University of Minnesota, 6-145 Jackson Hall, 321 Church St SE, Minneapolis, MN 55455, Phone: 1-612-625-6457, FAX: 1-612-626-5009, kofuj001@umn.edu.

Publisher's Disclaimer: This is a PDF file of an unedited manuscript that has been accepted for publication. As a service to our customers we are providing this early version of the manuscript. The manuscript will undergo copyediting, typesetting, and review of the resulting proof before it is published in its final citable form. Please note that during the production process errors may be discovered which could affect the content, and all legal disclaimers that apply to the journal pertain.

activity [17;18]. However, a more comprehensive characterization of the consequences of such mutations for Kir4.1 channel function has yet to be performed. In this study we report that SeSAME syndrome mutations cause variable loss of Kir4.1 channel function that can be rescued upon co-expression of wild-type Kir4.1 but not with Kir5.1 channels. Furthermore, almost all mutations do not largely impair the ability of these channels to be expressed at the plasma membrane indicating the potential utility of Kir channel openers for SeSAME syndrome therapy.

MATERIAL AND METHODS

Mutagenesis

The coding sequence of EGFP was fused in-frame to the N-terminus of rat Kir4.1 channel (plasmid generously provided by Dr. J. Adelman) and used as template for site-directed mutagenesis. Mutations were introduced using Quikchange II XL site-directed mutagenesis kit (Stratagene, Torrey Pines, CA) following the manufacturer's instructions. Rat Kir5.1 cDNA was a gift from Dr. Chun Jiang. The Kir5.1 coding sequence was transferred to pIRES2-DsRed-Express vector (Clontech, Mountain View, CA) to allow identification of Kir5.1-expressing cells. The coding sequences of all plasmids were confirmed by DNA sequencing.

Electrophysiology

HEK293 cells were grown in 35 mm dishes and transfected by using Polyfect reagent (Qiagen, Valencia, CA) with 2 μ g of plasmid per dish. One day post-transfection, HEK 293 cells were transferred to a recording chamber mounted on the stage of an upright microscope (E600 FN, Nikon, Tokyo, Japan) equipped with differential interference contrast optics and epifluorescence, which was used to localize EGFP- and some cases also DsRed-expressing cells. Recordings were performed using an Axon 700A Amplifier (Molecular Devices, Sunnyvale, CA), with extracellular solution containing (in mM): 140 NaCl, 5.0 KCl, 1.0 MgCl₂, 1.8 CaCl₂, 0.33 NaH₂PO₄, 10 glucose and 10 HEPES (pH adjusted to 7.3 with NaOH). Recordings were made with fire-polished borosilicate pipettes filled with: 125 KGlucuronate, 2 CaCl₂, 2 MgCl₂, 10 EGTA, 10 HEPES, 0.5 NaGTP, and 2 Na₂ATP, pH with KOH (pH 7.2). Current and voltage acquisitions were performed with a Digidata 1322 D/A and A/D converter (Molecular Devices) connected to a personal computer running pClamp 10 software (Molecular Devices). Liquid junction potentials between the bath and electrode were calculated using the Liquid Junction Potential Calculator in pClamp 10 (Molecular Devices) and were corrected in all recordings.

Whole cell currents were analyzed off-line with Clampfit (Molecular Devices). Resting membrane potential (RMP) values were measured immediately following whole-cell access. Cell capacitance (Cm) and input resistance were calculated from those currents evoked by stepping the cell potential to a 10 mV hyperpolarized value for 20 ms from a holding potential of -60 mV. Charge Q was estimated by time integration of evoked current during the step voltage. Input resistance was estimated from the steady-state evoked current during the step voltage.

Biotinylation of Cell Surface Proteins and Western Blots

Biotinylation of cell surface proteins was performed using the Pierce cell surface protein isolation kit (Thermo Scientific, Rockford, IL). Briefly, HEK293 cells were grown in 25 cm² flasks and transfected using Polyfect reagent (Qiagen, Valencia, CA) with 4 μ g of plasmid per flask. Cells were washed extensively with ice-cold Phosphate Buffered Saline (PBS) and incubated with Sulfo-NHS-SS-Biotin for 30 minutes at 4°C with gentle agitation. Unbound biotin was quenched with 500 μ l quenching solution supplied in the kit and cells

lyzed with 300 μ l RIPA buffer consisting of 50 mM Tris (pH 8.0), 150 mM NaCl, 50 mM EGTA, 1% Triton X-100, 0.1 % Sodium Dodecyl Sulfate, 0.5% Na Deoxycholate plus Complete protease inhibitor mixture (Roche, Indianapolis, IN) for 30 minutes at 4°C with constant agitation. Following centrifugation at 16000 X g, the supernatant was incubated with 300 μ l NeutrAvidin agarose for 1 hour at room temperature. The agarose was then washed to remove any unbound protein. Proteins bound to agarose were eluted using 50mM DTT in RIPA buffer by heating for 5 minutes at 95°C. Eluted proteins were stored at -80°C and used for Western blots.

For Western Blots, 24 μ g of eluted proteins were loaded and subjected to electrophoresis on NuPage 4–12% Bis-Tris gels (Invitrogen, Carlsbad, CA). Proteins were transferred to Invitrolon PVDF membranes (0.45 μ m pore size) for 2 hours at room temperature. The membranes were then blocked for 1 hour at room temperature with PBS + 0.2% Tween + 5% milk followed by incubation in either mouse-anti-EGFP (1:750, Clontech, Mountain View, CA) or mouse-anti-Na⁺/K⁺ ATPase (1:2000, Millipore, Billerica, MA) antibodies in PBS + 0.2% Tween + 1% milk overnight at 4°C with constant agitation. Membranes were washed extensively with PBS + 0.2% Tween + 1% Milk and the secondary antibody, HRP-anti-mouse (1:30,000), was added for one hour at room temperature. Following membrane washes with PBS + 0.2% Tween and PBS, immunoreactive bands were visualized by chemiluminescence (Lumi-Light, Roche).

Statistics

Numerical values are given as mean \pm SE. All comparisons across conditions for the same datasets were made using Student's t-test.

RESULTS

To determine the functional consequences of SeSAME syndrome mutations, we transfected HEK293 cells with expression vectors containing either wild-type or mutant Kir4.1 cDNAs (2 μ g/plate). The enhanced Green Fluorescent coding sequence was fused in frame to the amino terminus of the Kir4.1 coding sequence to allow visualization of transfected cells (Figure 1A). Following one day post-transfection, whole-cell voltage clamp recordings were performed and membrane currents were measured upon voltage steps from -160 mV to +30 mV. At potentials positive to E_K (estimated at -78 mV) large barium-sensitive inward currents in cells transfected with wild-type Kir4.1 cDNA were detected (-341.5 ± 50.3 pA/pF, $n = 11$, measured at -140mV)(Figure 1C, Table 1). Untransfected cells displayed only significant outward currents due to expression of endogenous Kv channels [19](Figure 1B). The weak inward rectification profile and barium-sensitivity of inward currents are characteristic of Kir4.1 channel-mediated currents expressed in heterologous expression systems [20; 21]. For Kir4.1 mutants, on the other hand, we observed diminished currents and variable loss of Kir4.1 channel function depending on the mutated residue (Figure 2A). Expression of R65P and A167V yielded smaller Kir channel currents than wild-type (Figure 2B) (R65P, -5.2 ± 1.0 pA/pF $n=13$; A167V, -23.0 ± 3.8 pA/pF, $n=14$; WT, -341.5 ± 50.3 pA/pF)($P<0.05$) while the remaining mutants yielded no detectable Kir currents (Figure 2B) (Table 1). R65P and A167V mutant currents were mainly carried by K⁺ ions as inferred by the similar reversal potential to the wild type currents (R65P, -63.3 ± 1.6 mV, $n=13$; A167V, -66.9 ± 0.9 mV, $n=14$; WT, -68.4 ± 0.6 mV, $n=13$).

Because the SeSAME syndrome appears to be a monogenic recessive disease [17;18] we wanted to determine the effect of co-transfection of equal ratios of wild-type and mutant plasmids (1 μ g each/plate). As shown in Figure 3, in all cases, expression of the wild-type Kir4.1 channel allowed the rescue of the mutant channel. Barium sensitive currents are similar as the wild-type (Figure 3B). Kir current density of transfected cells with mutant

Kir4.1 channels was not significantly different than those transfected with wild-type Kir4.1 channels ($p > 0.05$ compared with the wild-type Kir4.1) (Table 1). These results indicate that SeSAME mutations do not exert a dominant negative effect upon co-expression with wild-type Kir4.1 and that heteromeric assemblies of mutant and wild-type channels are probably fully functional, explaining the lack of a visible phenotype in heterozygous carriers for SeSAME syndrome [17].

Kir4.1 channels in diverse tissues such as kidney, retina and brain are thought to hetero-oligomerize with Kir5.1 channels [9;22;23;24], which by themselves do not generate functional channels [22]. To test whether Kir5.1 channels are able to “rescue” the function of mutant Kir4.1 channels we co-transfected equal ratios of Kir5.1 and mutant Kir4.1 channels (1 μ g each/plate) (Supplemental Figure S1). Overall, the current profiles obtained under these conditions were similar from those obtained with the homomeric channels (R297C, C140R, R199X, T164I). Again only R65P and A167V mutants yielded functional currents while the other Kir4.1 mutants failed to yield any functional currents despite the Kir5.1 channel co-expression (Table 1).

While the previous results indicate the loss of Kir4.1 channel function from various SeSAME mutations they do not provide insights into whether these mutations affect channel gating or cell surface membrane expression. Confocal images of transfected cells show EGFP fluorescence localized principally to intracellular compartments (data not shown) though we were unable to discern the presence of Kir4.1 channel mutants in the plasma membrane based on our cell imaging procedures. We therefore adopted a biochemical approach using cell-surface biotinylation experiments ($n=3$) to confirm the membrane localization of SeSAME syndrome channel mutants. The biotinylated surface proteins from transfected HEK293 cells were collected and processed by SDS-PAGE and visualized via Western analysis using an antiserum to the EGFP-epitope. Cell lysates were also processed by SDS-PAGE and visualized via Western analysis for EGFP to confirm equivalent protein loading. A representative Western blot of biotinylated Kir4.1 channel mutants is reported in Figure 4 as obtained 24 hrs following transfection in register with previous functional physiological experiments. The anti-EGFP antibody detected one distinct band of apparent molecular mass of 140 KDa which is likely to represent the dimeric form of the channel protein. The molecular mass of predicted Kir4.1-EGFP polypeptide is 70KDa, thus the low electrophoretic mobility of Kir4.1 likely reflects our failure to disaggregate the tetrameric channel protein. Similar low electrophoretic mobility for Kir4.1 in Western blots has been described previously for Kir4.1 channels [25]. We detected cell surface expression for the R65P, A167V, R297C, C140R, and T164I mutants (Figure 4). One notable exception was the lack of surface expression for the R199X non-sense mutation. Identical procedures with the exception of omission of biotinylation reagents failed to reveal any surface expression confirming the specificity of the assay.

DISCUSSION

Channelopathies have provided an unique window on the fundamental biology and functions of various channels in diverse cell types [26]. Kir-associated channelopathies have been linked to diseases affecting primarily renal, pancreatic or cardiac function [26]. The SeSAME syndrome is characterized by a constellation of seemingly unrelated multi-organ dysfunctions [17;18]. Patients with sensorineural deafness, epilepsy, ataxia and a renal salt-losing symptoms possess homozygous mutations in *KCNJ10*. The wide range of tissues affected in SeSAME syndrome reflects the extensive pattern of Kir4.1 channel tissue expression [27].

Using an amenable heterologous expression system we found that various SeSAME mutations affect Kir4.1 channel function dissimilarly. Two mutations (R65P and A167V) yielded productive Kir4.1 channel currents with overall properties similar to wild-type. Thus these mutant channels were sensitive to extracellular blockade by barium ions and were selective for K⁺. These currents were, however, considerably smaller than those measured in the wild-type channel. The remaining SeSAME mutations, R297C, C120R, R199X and T164I yielded currents too small to resolve in our electrophysiological assays. Even by raising extracellular K⁺ to 50 mM to maximize the magnitude of inward currents we were not able to detect the expression of these mutant channels (data not shown). Previous studies performed on Kir4.1 channels or other members of Kir channel family provide some insights into the functional consequences of these mutations. Neutralization of positively charged residues at R65 and R297 is likely to affect the PIP₂ binding to the channel, an essential cofactor for gating in the Kir channel family [28]. The more mild effect of R65 neutralization may indicate that residual PIP₂ binding persists in these mutant channels. A step subsequent to PIP₂ binding may be affected in the T164I mutant as this particular mutation prevents the formation of H-bonds between the channel two transmembrane helices (TM) [29] and affect channel gating [29]. The cysteine residue at position 120 in Kir4.1 is conserved across other Kir channel family members and mutation of this residue in the homologous Kir2.3 channel induced a loss of channel function [30].

In SeSAME syndrome, the wide array of tissue dysfunctions is only manifested in homozygous patients and such lack of dominant negative effect of the disease-causing mutations was recapitulated in our study where co-expression of mutant and wild-type channels resulted in wild-type like currents. The apparent haplosufficiency of KCNJ10 is also seen in Kir4.1 knockout mouse models in which the heterozygous animals do not bear gross behavioral or reproductive abnormalities [15]. It is somewhat surprising that we did not observe a dominant-negative effect for the C120R mutation in our experiments as expression of the analogous mutation in Kir2.3 channels was reported to show a dominant negative inhibition of wild-type currents in *Xenopus* oocytes [30]. We speculate that differences in post-translational processing of proteins in these two expression systems might account for these discrepancies.

Our assessment of cell surface expression of the Kir4.1 channel mutants also reveal that missense mutations (R65P, A167V, R297C, C140R and T164I) did not drastically impair the ability of these channels to be expressed at the plasma membrane. Agents that induce or maintain the opening of Kir4.1 channels may therefore offer a potential avenue of therapy for patients bearing such mutations. However the diminished or lack of plasma membrane expression for the nonsense mutation R199X makes clear that development of novel therapies should be tailored to individual patients.

It is intriguing that SeSAME mutations which failed to yield functional expression in our studies do not cause early postnatal lethality in patients [17] while mutant mice with genetic inactivation of Kir4.1 do not survive beyond two or three weeks of age [15;31]. Species differences might account for such drastic differences in mortality rates or perhaps the inactive channels in many SeSAME syndrome patients may still have a functional role. Conceivably Kir4.1 mutants in the native tissue may be rescued partially by another accessory protein or even another Kir channel subunit. Further investigations using animal models of SeSAME syndrome might provide insights to these questions.

Supplementary Material

Refer to Web version on PubMed Central for supplementary material.

Acknowledgments

This work was supported in part by grants from the NIH R01EY012949, R21-EY018885.

References

1. Doupnik CA, Davidson N, Lester HA. The inward rectifier potassium channel family. *Curr Opin Neurobiol.* 1995; 5:268–77. [PubMed: 7580148]
2. Nichols CG, Lopatin AN. Inward rectifier potassium channels. *Annu Rev Physiol.* 1997; 59:171–91. [PubMed: 9074760]
3. Bichet D, Haass FA, Jan LY. Merging functional studies with structures of inward-rectifier K(+) channels. *Nat Rev Neurosci.* 2003; 4:957–67. [PubMed: 14618155]
4. Olsen ML, Sontheimer H. Functional implications for Kir4.1 channels in glial biology: from K⁺ buffering to cell differentiation. *J Neurochem.* 2008; 107:589–601. [PubMed: 18691387]
5. Butt AM, Kalsi A. Inwardly rectifying potassium channels (Kir) in central nervous system glia: a special role for Kir4.1 in glial functions. *J Cell Mol Med.* 2006; 10:33–44. [PubMed: 16563220]
6. Rozengurt N, Lopez I, Chiu CS, Kofuji P, Lester HA, Neusch C. Time course of inner ear degeneration and deafness in mice lacking the Kir4.1 potassium channel subunit. *Hear Res.* 2003; 177:71–80. [PubMed: 12618319]
7. Marcus DC, Wu T, Wangemann P, Kofuji P. KCNJ10 (Kir4.1) potassium channel knockout abolishes endocochlear potential. *Am J Physiol Cell Physiol.* 2002; 282:C403–7. [PubMed: 11788352]
8. Ito M, Inanobe A, Horio Y, Hibino H, Isomoto S, Ito H, Mori K, Tonosaki A, Tomoike H, Kurachi Y. Immunolocalization of an inwardly rectifying K⁺ channel, K_{AB}-2 (Kir4.1), in the basolateral membrane of renal distal tubular epithelia. *FEBS Letters.* 1996; 388:11–5. [PubMed: 8654579]
9. Lachheb S, Cluzeaud F, Bens M, Genete M, Hibino H, Lourdel S, Kurachi Y, Vandewalle A, Teulon J, Paulais M. Kir4.1/Kir5.1 channel forms the major K⁺ channel in the basolateral membrane of mouse renal collecting duct principal cells. *Am J Physiol Renal Physiol.* 2008; 294:F1398–407. [PubMed: 18367659]
10. Tang X, Schmidt TM, Perez-Leighton CE, Kofuji P. Inwardly rectifying potassium channel Kir4.1 is responsible for the native inward potassium conductance of satellite glial cells in sensory ganglia. *Neuroscience.* 166:397–407. [PubMed: 20074622]
11. Tang X, Taniguchi K, Kofuji P. Heterogeneity of Kir4.1 channel expression in glia revealed by mouse transgenesis. *Glia.* 2009; 57:1706–15. [PubMed: 19382212]
12. Connors NC, Kofuji P. Potassium channel Kir4.1 macromolecular complex in retinal glial cells. *Glia.* 2006; 53:124–31. [PubMed: 16206160]
13. Connors NC, Adams ME, Froehner SC, Kofuji P. The potassium channel Kir4.1 associates with the dystrophin glycoprotein complex via alpha-syntrophin in glia. *J Biol Chem.* 2004
14. Kofuji P, Biedermann B, Siddharthan V, Raap M, Iandiev I, Milenkovic I, Thomzig A, Veh RW, Bringmann A, Reichenbach A. Kir potassium channel subunit expression in retinal glial cells: implications for spatial potassium buffering. *Glia.* 2002; 39:292–303. [PubMed: 12203395]
15. Kofuji P, Ceelen P, Zahs KR, Surbeck LW, Lester HA, Newman EA. Genetic inactivation of an inwardly rectifying potassium channel (Kir4.1 subunit) in mice: phenotypic impact in retina. *J Neurosci.* 2000; 20:5733–40. [PubMed: 10908613]
16. Neusch C, Papadopoulos N, Muller M, Maletzki I, Winter SM, Hirrlinger J, Handschuh M, Bahr M, Richter DW, Kirchhoff F, Hulsmann S. Lack of the Kir4.1 channel subunit abolishes K⁺ buffering properties of astrocytes in the ventral respiratory group: impact on extracellular K⁺ regulation. *J Neurophysiol.* 2006; 95:1843–52. [PubMed: 16306174]
17. Scholl UI, Choi M, Liu T, Ramaekers VT, Hausler MG, Grimmer J, Tobe SW, Farhi A, Nelson-Williams C, Lifton RP. Seizures, sensorineural deafness, ataxia, mental retardation, and electrolyte imbalance (SeSAME syndrome) caused by mutations in KCNJ10. *Proc Natl Acad Sci U S A.* 2009; 106:5842–7. [PubMed: 19289823]
18. Bockenbauer D, Feather S, Stanescu HC, Bandulik S, Zdebik AA, Reichold M, Tobin J, Lieberer E, Sterner C, Landoure G, Arora R, Sirimanna T, Thompson D, Cross JH, van't Hoff W, Al Masri

- O, Tullus K, Yeung S, Anikster Y, Klootwijk E, Hubank M, Dillon MJ, Heitzmann D, Arcos-Burgos M, Knepper MA, Dobbie A, Gahl WA, Warth R, Sheridan E, Kleta R. Epilepsy, ataxia, sensorineural deafness, tubulopathy, and KCNJ10 mutations. *N Engl J Med*. 2009; 360:1960–70. [PubMed: 19420365]
19. Jiang B, Sun X, Cao K, Wang R. Endogenous Kv channels in human embryonic kidney (HEK-293) cells. *Mol Cell Biochem*. 2002; 238:69–79. [PubMed: 12349911]
 20. Horio Y, Hibino H, Inanobe A, Yamada M, Ishii M, Tada Y, Satoh E, Hata Y, Takai Y, Kurachi Y. Clustering and enhanced activity of an inwardly rectifying potassium channel, Kir4.1, by an anchoring protein, PSD-95/SAP90. *J Bio Chem*. 1997; 272:12885–8. [PubMed: 9148889]
 21. Takumi T, Ishii T, Horio Y, Morishige K, Takahashi N, Yamada M, Yamashita T, Kiyami H, Sohmiya K, Nakanishi S, Kurachi Y. A novel ATP-dependent inward rectifier potassium channel expressed predominantly in glial cells. *J Biol Chem*. 1995; 270:16339–46. [PubMed: 7608203]
 22. Tanemoto M, Kittaka N, Inanobe A, Kurachi Y. In vivo formation of a proton-sensitive K⁺ channel by heteromeric subunit assembly of Kir5.1 with Kir4.1. *J Physiol*. 2000; 525(Pt 3):587–92. [PubMed: 10856114]
 23. Yang Z, Xu H, Cui N, Qu Z, Chanchevalap S, Shen W, Jiang C. Biophysical and molecular mechanisms underlying the modulation of heteromeric Kir4.1-Kir5.1 channels by CO₂ and pH. *J Gen Physiol*. 2000; 116:33–45. [PubMed: 10871638]
 24. Lourdel S, Paulais M, Cluzeaud F, Bens M, Tanemoto M, Kurachi Y, Vandewalle A, Teulon J. An inward rectifier K(+) channel at the basolateral membrane of the mouse distal convoluted tubule: similarities with Kir4-Kir5.1 heteromeric channels. *J Physiol*. 2002; 538:391–404. [PubMed: 11790808]
 25. Connors NC, Kofuji P. Dystrophin Dp71 is critical for the clustered localization of potassium channels in retinal glial cells. *J Neurosci*. 2002; 22:4321–7. [PubMed: 12040037]
 26. Abraham MR, Jahangir A, Alekseev AE, Terzic A. Channelopathies of inwardly rectifying potassium channels. *Faseb J*. 1999; 13:1901–10. [PubMed: 10544173]
 27. Bond CT, Pessia M, Xia XM, Lagrutta A, Kavanaugh MP, Adelman JP. Cloning and expression of a family of inward rectifier potassium channels. *Receptors Channels*. 1994; 2:183–91. [PubMed: 7874445]
 28. Lopes CM, Zhang H, Rohacs T, Jin T, Yang J, Logothetis DE. Alterations in conserved Kir channel-PIP₂ interactions underlie channelopathies. *Neuron*. 2002; 34:933–44. [PubMed: 12086641]
 29. Rapedius M, Paynter JJ, Fowler PW, Shang L, Sansom MS, Tucker SJ, Baukowitz T. Control of pH and PIP₂ gating in heteromeric Kir4.1/Kir5.1 channels by H-Bonding at the helix-bundle crossing. *Channels (Austin)*. 2007; 1:327–30. [PubMed: 18690035]
 30. Bannister JP, Young BA, Sivaprasadarao A, Wray D. Conserved extracellular cysteine residues in the inwardly rectifying potassium channel Kir2.3 are required for function but not expression in the membrane. *FEBS Lett*. 1999; 458:393–9. [PubMed: 10570947]
 31. Neusch C, Rozengurt N, Jacobs RE, Lester HA, Kofuji P. Kir4.1 potassium channel subunit is crucial for oligodendrocyte development and in vivo myelination. *J Neurosci*. 2001; 21:5429–38. [PubMed: 11466414]

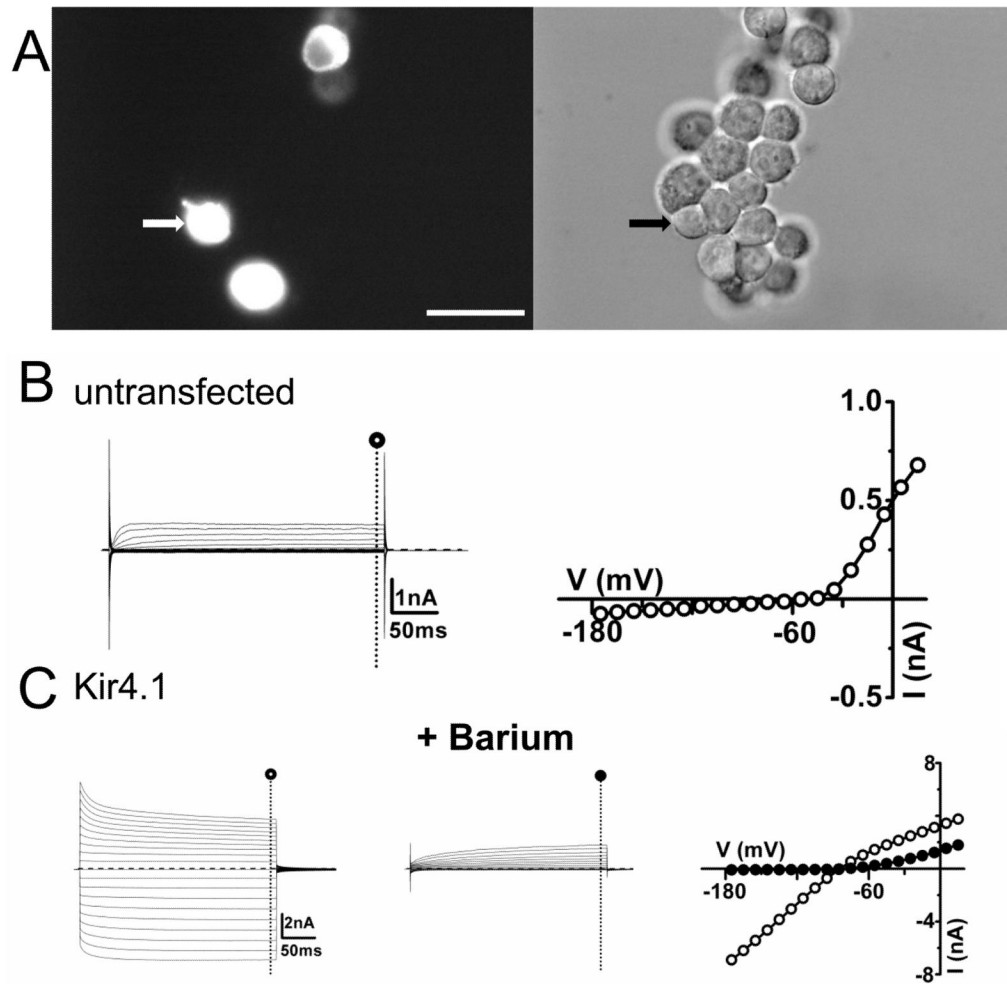


FIGURE 1. Expression of wild-type Kir4.1 channels in HEK 293 cells

(A) Left panel shows epifluorescence image of Kir4.1-expressing cells. DIC image of the same cells in the right panel with the recorded cell indicated by an arrow. (B) Representative currents and I - V relationships evoked by depolarization steps from a holding potential of -60 mV in 10 mV increments in untransfected HEK 293 cells. Current values were estimated at the end of the voltage pulse (\circ) (C) Representative current traces and I - V relationships for Kir4.1-EGFP transfected cell in the absence (\circ) and presence (\bullet) of $100\mu\text{M}$ barium in the bath. Scale bar: $50\mu\text{m}$ (A).

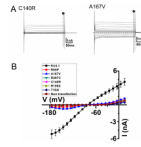


FIGURE 2. Partial or total loss of Kir4.1 currents for SeSAME syndrome mutant channels expressed in HEK 293 cells
(A) Macroscopic whole-cell currents of C140R or A167V currents evoked by a 300ms voltage commands from -160 to $+30$ mV. The holding potential was clamped at -60 mV.
(B) Average I - V relationships recorded from Kir4.1 wild-type and SesSAME syndrome mutant channels.

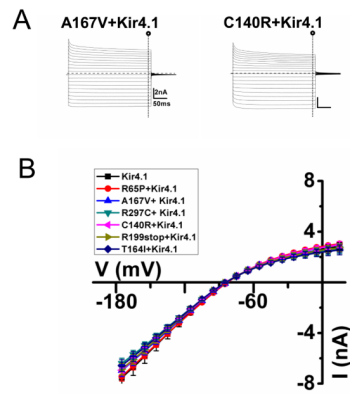


FIGURE 3. Rescue of Kir4.1 currents on co-expression of wild-type and SeSAME mutant Kir4.1 channels in HEK 293 cells

(A) Representative current traces for A167V, C140R co-transfected with wild-type Kir4.1 channel (C) Mean I - V relationships of barium-sensitive currents recorded from co-transfection of wild-type and mutant Kir4.1.

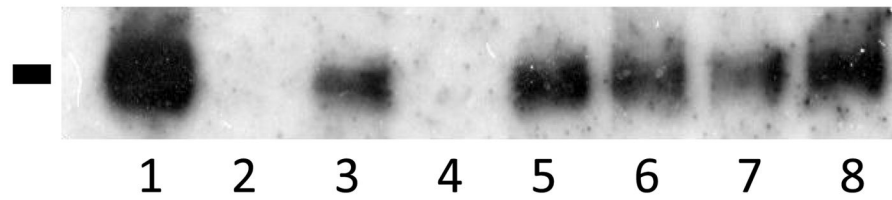


FIGURE 4. Surface expression of missense SeSAME syndrome mutant channel

A biotinylation assay was used to detect the surface expression of channel protein and representative Western blot is shown. Surface expression of Kir4.1 wild-type and mutant channels were detected with exception of the non-sense R199X mutation. Lanes: 1, Kir4.1; 2, Kir4.1 without biotin; 3, A167V; 4, R199X; 5, C140R; 6, T164I; 7, R65P; 8, R297C.

Table 1

Resting membrane potential (RMP), input resistance and current density of transfected Kir4.1 wild-type and mutants in HEK293 cells.

	number	RMP(mV)	Input Resistance(M Ω)	Current density (pA/pF, @-140mV)
untransfected	12	-36.8 \pm 2.5	1908.2 \pm 259.0	-1.8 \pm 0.2
Kir4.1	11	-68.4 \pm 0.6	24.0 \pm 4.2*	-341.5 \pm 50.3*
R65P	13	-63.3 \pm 1.6	572.5 \pm 165.8*	-5.2 \pm 1.0*
A167V	14	-66.9 \pm 0.9	160.5 \pm 24.8*	-23.0 \pm 3.8*
R297C	17	-34.9 \pm 1.2	2777.8 \pm 586.4 [†]	-2.4 \pm 0.3 [†]
C140R	15	-39.0 \pm 1.2	2543.0 \pm 806.2 [†]	-2.0 \pm 0.2 [†]
R199X	11	-35.6 \pm 1.6	1548.9 \pm 285.4 [†]	-2.5 \pm 0.4 [†]
T164I	13	-36.0 \pm 1.7	2404.2 \pm 295.9 [†]	-3.3 \pm 0.3 [†]
Kir4.1 +Kir4.1	12	-66.1 \pm 0.6	14.0 \pm 1.0	-354.2 \pm 26.3
R65P+Kir4.1	08	-66.3 \pm 0.3	16.3 \pm 2.5 [‡]	-341.3 \pm 30.4 [‡]
A167V+Kir4.1	11	-66.5 \pm 0.3	15.0 \pm 1.2 [‡]	-324.1 \pm 29.3 [‡]
R297C+Kir4.1	10	-66.6 \pm 0.3	16.2 \pm 1.2 [‡]	-333.3 \pm 32.5 [‡]
C140R+Kir4.1	09	-66.9 \pm 0.5	13.6 \pm 0.6 [‡]	-341.8 \pm 25.0 [‡]
R199X+ Kir4.1	11	-67.5 \pm 0.7	14.8 \pm 1.1 [‡]	-344.4 \pm 21.0 [‡]
T164I+ Kir4.1	11	-65.6 \pm 0.5	14.2 \pm 1.4 [‡]	-326.7 \pm 16.0 [‡]
Kir4.1+Kir5.1	12	-66.1 \pm 0.6	11.6 \pm 0.7	-366.2 \pm 21.4
R65P+ Kir5.1	10	-65.4 \pm 0.6	94.1 \pm 11.7 [§]	-51.1 \pm 12.3 [§]
A167V+ Kir5.1	08	-66.8 \pm 0.7	67.7 \pm 11.6 [§]	-83.3 \pm 9.6 [§]
R297C+Kir5.1	10	-39.9 \pm 2.2	1624.4 \pm 275.8 [§]	-3.7 \pm 0.4 [§]
C140R+Kir5.1	10	-35.9 \pm 1.6	2510.6 \pm 551.6 [§]	-2.0 \pm 0.4 [§]
R199X+ Kir5.1	08	-35.1 \pm 0.7	1794.9 \pm 381.8 [§]	-2.0 \pm 0.2 [§]
T164I+ Kir5.1	11	-38.5 \pm 1.9	1717.1 \pm 158.8 [§]	-3.8 \pm 0.4 [§]

* represents significant values (P< 0.05), when compared to the data obtained in untransfected group.

[†] represents no significant values (P>0.05), when compared to the data obtained in untransfected group.

[‡] represents no significant values (P>0.05), when compared to the data obtained in the wild-type group.

[§] represents no significant values (P>0.05), when compared to the data obtained in kir4.1-Kir5.1 cotransfection.